Pharmaceutical Sciences and Drug Design
ISSN: 3062-4428
2023, Volume 3, Page No: 67-85

Available online at: www.galaxypub.co/page/journals

Galaxy Publication

Xiaoyao Sanjie Decoction Suppresses Triple-Negative Breast Cancer through Quercetin-Mediated Inhibition of EZH2/AKT1: Insights from Network Pharmacology and In Vivo Validation

Julian Gray[1]*, Claire Roberts[1], Mason Scott[1]

[1]Department of Biotechnology, Faculty of Science, Nagoya University, Nagoya, Japan.

***E-mail** ✉ julian.gray.jp@gmail.com

Received: 02 December 2022; **Revised:** 27 February 2023; **Accepted:** 28 February 2023

ABSTRACT

Triple-negative breast cancer (TNBC) is an aggressive subtype of breast cancer with high mortality, representing a serious challenge to women's health worldwide. Xiaoyao Sanjie Decoction (XYSJD) has shown promising anti-TNBC effects, yet the molecular mechanisms behind its therapeutic activity remain largely unexplored. This study aimed to investigate the efficacy of XYSJD and its active compound quercetin in TNBC and to elucidate the underlying mechanisms of action. The chemical composition of XYSJD was characterized using ultra-high-performance liquid chromatography coupled with quadrupole-orbitrap mass spectrometry (UHPLC-Q Exactive HFX-MS). Network pharmacology, bioinformatics, and molecular docking approaches were employed to predict potential molecular targets and pathways associated with XYSJD activity. In vitro, the effects of XYSJD on TNBC cell proliferation, migration, invasion, and apoptosis were assessed using CCK-8, EdU, wound healing, transwell, Hoechst-PI staining, and flow cytometry assays. Western blotting was performed to validate target pathway modulation. In vivo antitumor activity was evaluated using a TNBC xenograft mouse model.

Nine major constituents of XYSJD were identified, and 206 potential targets relevant to TNBC were predicted. Bioinformatics analyses highlighted the EZH2/AKT1 signaling axis as a key pathway involved in XYSJD's anticancer activity, with apoptosis emerging as a primary biological process affected. Both XYSJD and quercetin significantly inhibited TNBC cell growth and induced apoptosis in vitro and in vivo. Mechanistically, quercetin suppressed TNBC progression by downregulating the EZH2/AKT1 pathway, whereas overexpression of EZH2 or AKT1, or activation of AKT via SC79, attenuated quercetin-induced apoptosis. XYSJD exhibits potent antitumor effects against TNBC, with quercetin acting as a principal bioactive compound that triggers apoptosis through inhibition of the EZH2/AKT1 pathway. These findings provide a mechanistic rationale for the potential clinical application of XYSJD in TNBC therapy.

Keywords: Xiaoyao Sanjie Decoction, Triple-negative breast cancer, Quercetin, Network pharmacology, EZH2/AKT1 signaling pathway

How to Cite This Article: Gray J, Roberts C, Scott M. Xiaoyao Sanjie Decoction Suppresses Triple-Negative Breast Cancer through Quercetin-Mediated Inhibition of EZH2/AKT1: Insights from Network Pharmacology and In Vivo Validation. Pharm Sci Drug Des. 2023;3:67-85. https://doi.org/10.51847/PVhsZss9W8

Introduction

Breast cancer (BC) represents the most frequently diagnosed malignancy among women globally and remains a leading cause of cancer-related mortality [1]. Triple-negative breast cancer (TNBC) accounts for approximately 15–20% of all BC cases [2, 3]. Compared with other BC subtypes, TNBC is characterized by poor differentiation, higher aggressiveness, and a propensity for metastasis, with around 46% of patients developing distant metastases [4, 5]. The absence of estrogen receptor (ER), progesterone receptor, and human epidermal growth factor receptor 2 (HER2) in TNBC limits the effectiveness of targeted therapies against ERα or HER2 [6, 7]. At present, surgery combined with systemic chemotherapy constitutes the standard treatment strategy for TNBC [8, 9]; however, these approaches are often insufficient for patients with recurrent or metastatic disease [10], resulting in shorter

overall survival compared with other BC subtypes [11]. Consequently, TNBC continues to pose significant clinical challenges. Complementary therapies, including Traditional Chinese Medicine (TCM), are increasingly being explored as potential adjunctive or alternative strategies for TNBC management [12, 13].

Xiaoyao Sanjie Decoction (XYSJD), also referred to as Ruyan Sanjie Decoction, was developed by Professor Li Jiageng and is widely used in TCM for TNBC treatment. The formulation consists of Radix Bupleuri, Radix Paeoniae Rubra, Poria cocos, Angelica sinensis, Hedyotis diffusa, Prunella vulgaris L., Astragalus membranaceus, Curcuma zedoaria, and licorice. Previous studies indicate that the basic Xiaoyao Powder prescription can inhibit BC growth and improve related clinical symptoms [14–17]. Several constituents of XYSJD demonstrate specific anti-TNBC effects; for instance, Saikosaponin D from Radix Bupleuri suppresses TNBC cell proliferation via β-catenin signaling [18], while Paeoniflorin from Radix Paeoniae Rubra inhibits hypoxia-induced epithelial–mesenchymal transition in MDA-MB-231 cells through the PI3K/Akt/HIF-1α pathway [19]. Isoliquiritigenin, derived from licorice, also exhibits anticancer activity against TNBC [20].

According to TCM principles, blood stasis contributes significantly to tumor progression [21, 22]. Based on this concept, blood-activating and stasis-removing herbs such as Hedyotis diffusa, Curcuma zedoaria, and Prunella vulgaris L. are incorporated into XYSJD. Methylanthraquinone from Hedyotis diffusa can inhibit cell proliferation, disrupt mitochondrial integrity, and induce apoptosis in MCF-7 cells [23]. Curcuma zedoaria extract has been reported to limit TNBC invasion and metastasis [24], while Prunella vulgaris L. extracts inhibit proliferation and promote apoptosis in BC models [25]. Quercetin, a flavonol commonly found in fruits, vegetables, and TCM, has shown notable anti-TNBC activity [26, 27] and is a critical bioactive component present in several XYSJD ingredients, including Radix Paeoniae Rubra, Hedyotis diffusa, Prunella vulgaris L., Astragalus membranaceus, and licorice [28–34]. Based on these observations, we hypothesize that quercetin may serve as the principal active compound in XYSJD for TNBC treatment, which will be further validated using network pharmacology and UHPLC-Q Exactive HFX-MS.

Unlike single-compound treatments, TCM prescriptions such as XYSJD exert therapeutic effects through multiple components, targets, and pathways, making their mechanisms complex and not fully understood. Network pharmacology provides a framework for mapping the intricate “drug–target–disease” interactions, facilitating identification of active compounds and prediction of underlying molecular mechanisms at the level of gene function, molecular interaction, and signaling pathways [35]. In this study, we combined network pharmacology and bioinformatics approaches to pinpoint key targets and signaling pathways of XYSJD against TNBC, analyzed the expression and clinical relevance of these targets, and evaluated compound-target interactions using molecular docking. Finally, the anti-TNBC effects and mechanisms of XYSJD and its active components were confirmed through in vitro and in vivo experiments. The workflow of the study is summarized in **Figure 1**.

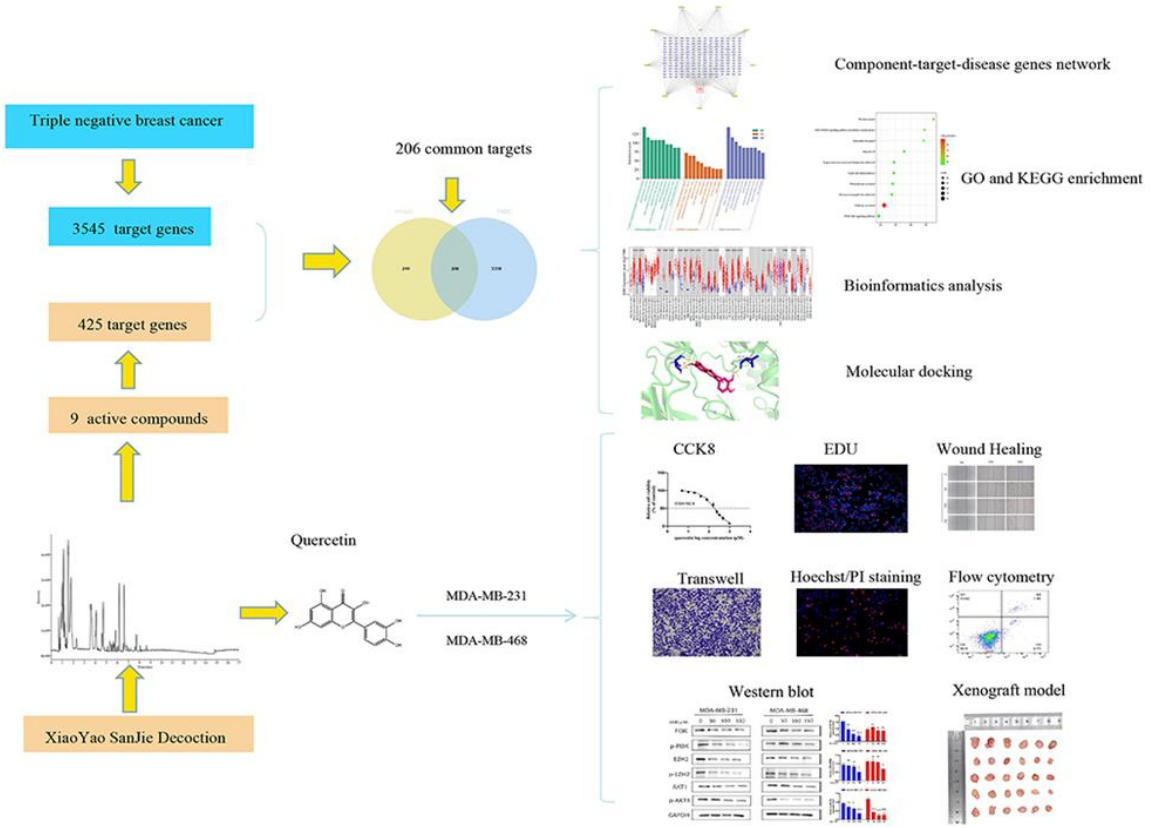

Figure 1. The flow chart of the study.

Materials and Methods

Network pharmacology and bioinformatics analysis of XYSJD for TNBC

Analysis of XYSJD constituents via UHPLC-Q exactive HFX-MS

XYSJD granules (100 mg) were accurately weighed into a centrifuge tube and homogenized with 0.1 mL precooled water for 60 seconds. Subsequently, 0.4 mL of an extraction solution (acetonitrile–methanol, 1:1, v/v) was added, homogenized for 60 seconds, and subjected to two cycles of low-temperature ultrasonication for 30 minutes. The mixture was incubated at −20°C for 1 hour to precipitate proteins, followed by centrifugation at 12,000 rpm for 10 minutes at 4°C. The resulting supernatant was dried under vacuum, reconstituted in 200 µL of 30% acetonitrile, homogenized, and centrifuged at 14,000 rpm for 15 minutes at 4°C. The final supernatant was collected for analysis.

Chromatographic separation was performed on a Waters HSS T3 column (100 × 2.1 mm, 1.8 µm) at 40°C with a flow rate of 0.3 mL/min and an injection volume of 2 µL. The mobile phase consisted of Milli-Q water with 0.1% formic acid (phase A) and an isopropyl alcohol–acetonitrile mixture with 0.1% formic acid (phase B). The gradient program was as follows: 0–2 min, 90:10 (A:B); 2–6 min, 40:60 (A:B); 6–15 min, 40:60 (A:B); 15.1–17 min, 90:10 (A:B).

High-resolution mass spectrometry (HRMS) was conducted on a Q Exactive HFX Hybrid Quadrupole-Orbitrap instrument (Thermo Fisher Scientific) equipped with a heated ESI source using the Full-MS-ddMS2 acquisition mode. The source parameters were set as: sheath gas 40 arb, auxiliary gas 10 arb, spray voltage +3000 V / −2800 V, capillary temperature 350°C, and ion transport tube temperature 320°C. The primary mass scan range was 70–1050 m/z with a resolution of 70,000 for MS1 and 17,500 for MS2. Raw data were acquired using Xcalibur 4.1 and processed with Progenesis QI (Waters Corporation) for baseline correction, peak detection, retention time alignment, and peak intensity extraction. Compound identification was conducted using a self-built TCM secondary mass spectrometry database, with MS1 mass error <15 ppm and MS2 fragment similarity >0.7.

Identification of active compounds and corresponding targets

To identify biologically active compounds, thresholds of oral bioavailability (OB) ≥30% [36] and drug-likeness (DL) ≥0.18 [37] were applied via the TCMSP database (https://tcmspw.com/tcmsp.php). The SMILES structures

of each active compound were obtained from PubChem (https://pubchem.ncbi.nlm.nih.gov/) and used for target prediction on SwissTargetPrediction (https://www.swisstargetprediction.ch/) with "Homo sapiens" as the species. Targets were standardized to gene IDs using the UniProt database (https://www.uniprot.org/).

Identification of potential TNBC targets for XYSJD

TNBC-related targets were retrieved from GeneCards (https://www.genecards.org/) and OMIM (https://www.omim.org/) using "Triple-negative breast cancer" as the keyword and restricting to Homo sapiens. Jvenn (http://www.bioinformatics.com.cn/static/others/jvenn/example.html) was employed to identify overlapping targets between XYSJD compounds and TNBC-related genes, which were considered potential therapeutic targets.

Construction of the XYSJD–compound–target–TNBC network and PPI analysis

The active compounds and intersecting targets were imported into Cytoscape 3.8.0 to construct the "XYSJD–compound–target–TNBC" network. Protein-protein interaction (PPI) analysis was performed using STRING (https://string-db.org/) with appropriate confidence score filtering. The resulting interaction data were visualized in Cytoscape, and cytoHubba was employed to identify central hub proteins using multiple topological algorithms.

GO and KEGG enrichment analysis

The common target genes were analyzed for Gene Ontology (GO) and Kyoto Encyclopedia of Genes and Genomes (KEGG) pathway enrichment using Metascape (https://metascape.org/gp/index.html#/main/step1) with significance thresholds of $P < 0.01$ and FDR < 0.01. The results were visualized using the bioinformatics online platform (www.bioinformatics.com.cn).

Gene expression and prognostic analysis

Differential expression of AKT1 and EZH2 in tumor versus adjacent normal tissues was assessed using TIMER2.0 (http://timer.comp-genomics.org/), and their correlation was analyzed using GEPIA2 (http://gepia2.cancer-pku.cn/#index). Expression patterns across BC subtypes, TNBC, disease stage, and metastasis were explored via UALCAN (https://ualcan.path.uab.edu/cgi-bin/ualcan-res.pl) and GSE65194. Kaplan-Meier survival analysis was performed using GSE21653, with $P < 0.05$ considered significant. The study was approved by the Institutional Review Board of Hubei University of Science and Technology (IACUC-202410001).

Molecular docking

Based on the PPI network and KEGG analysis, AKT1 (PDBID: 3O96) and EZH2 (PDBID: 4MI5) were selected as target receptors. The 3D structures were obtained from the Protein Data Bank (http://www.rcsb.org), and processed in PyMOL 3.8 for dewatering and ligand removal. Quercetin was selected as the ligand (mol2 format, TCMSP) and prepared using AutoDock Tools for hydrogenation and charge assignment. Binding affinities were calculated using AutoDock Vina (http://vina.scripps.edu/), and docking conformations were visualized in PyMOL.

Experimental verification

XYSJD preparation and animal serum collection

The herbal granules comprising Xiaoyao Sanjie Decoction (XYSJD) were procured from Hubei Tianji Pharmaceutical Co., Ltd. The granules were dissolved in boiling distilled water and concentrated to achieve a stock solution of 2 g/mL.

Female Sprague Dawley rats (8 weeks old, 250 ± 20 g) were obtained and housed under controlled conditions: 12-hour light/dark cycle, 25°C ambient temperature, and 55% humidity, with three animals per cage. Following one week of acclimation, rats were randomly assigned to either the XYSJD treatment group or a control group. The treatment group received XYSJD orally at a dose of 6 g/kg, administered twice daily for three consecutive days, while the control group received an equal volume of distilled water.

One hour after the final dose, animals were anesthetized with 2% pentobarbital sodium (30 mg/kg, intraperitoneally). Blood was collected from the abdominal aorta and left to clot at room temperature for approximately 60 minutes. Rats were then euthanized via cervical dislocation. Serum was isolated by

centrifugation at 3,000 rpm for 15 minutes, heat-inactivated at 56°C, filtered through a 0.22-μm membrane, and stored at −80°C for further experiments.

All procedures complied with institutional guidelines and ethical standards for animal research, as approved by the Institutional Animal Care and Use Committee of Huazhong University of Science and Technology (IACUC approval number: IACUC-2022-3324). The experiments conformed to national regulations and international principles governing laboratory animal welfare.

Table 1. Herbal Formula of XYSJ

Latin Name of the Medicinal Material	Material	Chinese Name	Dose (g)
Radix bupleuri	root	Chai Hu	10
Radix Paeoniae Rubra	root	Chi Shao	10
Poria cocos	sclerotium	Fu Ling	10
Angelica sinensis	root	Dang Gui	10
Hedyotis Diffusa	herb	Bai Hua She She Cao	15
Prunella vulgaris L	fruiting spikes	Xia Ku Cao	10
Astragalus Membranaceus	rootstalk	Huang Qi	10
Curcuma zedoaria	rootstalk	EZhu	15
Licorice	root and rootstal	Gan Cao	6

Cell lines and reagents

The human triple-negative breast cancer (TNBC) cell lines, MDA-MB-231 and MDA-MB-468, were obtained from Wuhan Pricella Biotechnology Co., Ltd. (China). Quercetin (≥95% purity; SQ8030) was supplied by Beijing Solarbio Science & Technology Co., Ltd. (Beijing, China), and SC-79, an AKT activator, was purchased from Beyotime (Shanghai, China). Cells were maintained in DMEM (Servicebio, China) supplemented with 10% fetal bovine serum (FBS, MeiSenCTCC, China) under standard culture conditions (37°C, 5% CO_2, humidified incubator). Morphological assessments were performed periodically to ensure cellular integrity and growth.

Cell viability assessment

MDA-MB-231 and MDA-MB-468 cells were seeded at 4×10^4 cells/mL into 96-well plates and incubated for 12 h to allow adherence. Cells were then exposed to a series of XYSJD concentrations (0%, 5%, 10%, 15%, 20%) for 48 and 72 h. In parallel, blank rat serum was applied at concentrations of 0%, 5%, 10%, 15%, and 20% to maintain a consistent final serum content of 20% across all groups. For quercetin treatments, cells were incubated with increasing concentrations (0–960 μM) under identical conditions. Following 48 h of treatment, 10 μL of CCK-8 reagent (Beyotime, China) was added to each well, incubated for 1 h, and absorbance was measured at 450 nm using a microplate reader (PerkinElmer, EnSpire, USA).

EdU cell proliferation assay

Cells were plated into 96-well plates and treated with quercetin at 0, 50, 100, and 150 μM for 24 h. Proliferation was assessed using the BeyoClick™ EdU Cell Proliferation Kit (Alexa Fluor 594, Beyotime, China). Cells were incubated with 10 μM EdU for 2 h, fixed with 4% paraformaldehyde, permeabilized with 0.3% Triton X-100, and subjected to the click reaction for 30 min in the dark at room temperature. Nuclei were counterstained with Hoechst 33258 for 10 min and visualized using a fluorescence microscope (IX51, Olympus, Japan).

Wound healing assay

Cells were seeded in 12-well plates and cultured overnight. A scratch was generated using a 200-μL pipette tip, followed by treatment with quercetin (0, 50, 100, 150 μM) in DMEM containing 5% FBS. Migration into the wound area was monitored at 0, 24, and 48 h and imaged with an inverted fluorescence microscope.

Transwell migration and invasion assays

For migration studies, MDA-MB-231 cells (3×10^4/well) and MDA-MB-468 cells (4×10^4/well) were seeded in the upper chambers of transwell inserts with serum-free medium, while the lower chambers contained medium

with 10–20% FBS. After 24 h, migrated cells were fixed with 4% paraformaldehyde, stained with 0.1% crystal violet, and imaged. For invasion assays, the upper chambers were pre-coated with a Matrigel dilution (1:3) and solidified at 37°C for 3 h before seeding cells. The procedure for staining and imaging followed the migration assay.

Apoptosis analysis

Cells treated with quercetin for 48 h were collected, washed, and resuspended in 500 µL of binding buffer. Annexin V-FITC (5 µL) and PI (5 µL) were added, incubated in the dark for 15 min, and analyzed using a CytoFLEX flow cytometer (Becton Dickinson, USA).

Hoechst/PI nuclear staining

Cells were seeded in 48-well plates, treated with quercetin for 48 h, washed with PBS, and incubated with Hoechst 33342 and PI for 15 min in the dark. Fluorescence imaging was performed with an inverted microscope.

Plasmid and siRNA transfection

MDA-MB-231 and MDA-MB-468 cells were transfected with either pcDNA3.1(+)-EZH2, pcDNA3.1(+)-control vector, or AKT1 siRNA using Lipofectamine 3000 and Opti-MEM, following the manufacturer's instructions. After 6 h, the transfection medium was replaced with fresh medium, and cells were incubated for 24 h before further treatments. Transfection efficiency was confirmed using RT-qPCR and Western blotting.

RNA isolation and RT-qPCR

Total RNA was extracted using Trizol reagent and quantified with a NANODROP ONEc spectrophotometer. cDNA synthesis was performed using Primescript RT Master Mix (Takara Bio, China). Quantitative PCR was conducted on a StepOnePlus system (Applied Biosystems, USA) with β-actin as an internal reference. Relative expression of EZH2 and AKT1 was calculated using the 2^−ΔΔCt method. All assays were performed in triplicate. Primers were synthesized by Shanghai Sangon Biotechnology (China) **(Table 2)**.

Table 2. The List of Primers and siRNA Sequence

Gene	Forward Primer	Reverse Primer
β-ACTIN	CATGTACGTTGCTATCCAGGC	CTCCTTAATGTCACGCACGAT
EZH2	CAGTTCGTGCCCTTGTGTGATAG	CTCTCGGACAGCCAGGTAGC
AKT1	AGGATGTGGACCAACGTGAGG	GCAGGCAGCGGATGATGAAG
Sequences for siRNA		
AKT1	CUAUGGCGCUGAGAUUGUGUCdTdT	GACACAAUCUCAGCGCCAUAGdTdT

Western blot analysis

TNBC cells were lysed using RIPA buffer containing PMSF (Servicebio, China) after 48 hours of treatment or transfection with different concentrations of quercetin. The lysates were centrifuged to collect the supernatant, and protein concentrations were quantified using a BCA assay (Beyotime, China). Equal amounts of protein (10 µg per lane) were separated by SDS-PAGE (Servicebio, China) and transferred to PVDF membranes trimmed to appropriate sizes based on molecular weight. Membranes were blocked with 5% nonfat milk for 1 hour and incubated overnight at 4°C with primary antibodies targeting PI3K p110β, phosphorylated PI3K p85α, AKT1, phosphorylated AKT1 (Abways, China; 1:1000), EZH2, phosphorylated EZH2 (ABclonal, China; 1:1000), and GAPDH (Abways, China; 1:3500). The following day, membranes were washed three times with TBST and incubated with goat anti-rabbit IgG secondary antibody (Abways, China; 1:10000) for 1 hour at room temperature, followed by three additional TBST washes (10 min each). Protein bands were detected using a ChemiScope 6200 gel imaging system (CLINX, China), and the gray values were quantified using ImageJ software, with GAPDH serving as the loading control.

Animal experiments

Thirty female BALB/c-nu mice (4 weeks old, 18–22 g) were obtained from Shulaibao (Wuhan) Biotechnology Co., Ltd. (Hubei, China). Following a 7-day acclimation, 5×10^6 MDA-MB-231 cells suspended in 50 µL PBS

and 50 μL Matrigel were subcutaneously injected into the right flank of each mouse to establish xenograft tumors. When tumor volumes reached approximately 100 mm^3, mice were randomly assigned to five treatment groups (n=6 per group): Control (saline 0.1 mL/kg), Cisplatin (2 mg/kg, intraperitoneal every 2 days), XYSJD (0.1 mL/kg, oral daily), Que 80 mg/kg (intraperitoneal daily), and Que 40 mg/kg (intraperitoneal daily). Treatments continued for 21 days, with tumor volume and body weight measured every three days. Twelve hours after the final administration, mice were euthanized by cervical dislocation. Tumors were excised, photographed, and weighed, and liver and kidney tissues were collected, fixed in 4% paraformaldehyde, and processed for hematoxylin and eosin (H&E) staining.

Statistical analysis

All results are expressed as mean ± standard deviation (SD). Statistical analyses were performed using GraphPad Prism 10.1.2. Comparisons between two groups were analyzed using Student's t-test, whereas differences among multiple groups were assessed using one-way ANOVA. Statistical significance thresholds were set at $P < 0.05$, $P < 0.01$, and $P < 0.001$.

Results and Discussion

Identification of active compounds and mechanistic insights of XYSJD against TNBC

UHPLC-Q Exactive HFX-MS analysis **(Figure 2)** identified nine compounds in XYSJD that met the screening criteria of OB ≥30% and DL ≥0.18 **(Table 3)**, corresponding to 425 predicted targets. After removing duplicates using GeneCards and OMIM, 3545 TNBC-related genes were obtained. Intersection analysis using Jvenn revealed 206 overlapping targets potentially mediating the effects of XYSJD against TNBC **(Figure 3a)**. A compound-target network was constructed, comprising 217 nodes and 663 edges **(Figure 3b)**. Degree analysis indicated that quercetin (degree = 82) may be a primary bioactive compound in XYSJD. PPI network analysis in STRING followed by cytoHubba topological analysis in Cytoscape identified the top 10 hub genes, with TP53 and AKT1 exhibiting the highest connectivity **(Figures 3c and 3d)**.

Table 3. 9 Bioactive Compounds of XYSJD

MOL ID	Metabolite	Retention time(min)	OB(%)	DL	Degree
MOL000098	Quercetin	5.614	46.43	0.28	82
MOL000422	Kaempferol	7.970	41.88	0.24	75
MOL002714	Baicalein	6.475	33.52	0.21	57
MOL002565	Medicarpin	8.743	49.22	0.34	55
MOL000006	Luteolin	9.672	36.16	0.25	55
MOL004908	Glabridin	10.386	53.25	0.47	54
MOL000279	Cerevisterol	12.373	37.96	0.77	50
MOL000417	Calycosin	7.323	47.75	0.24	23
MOL004912	Glabrone	10.439	52.51	0.50	6

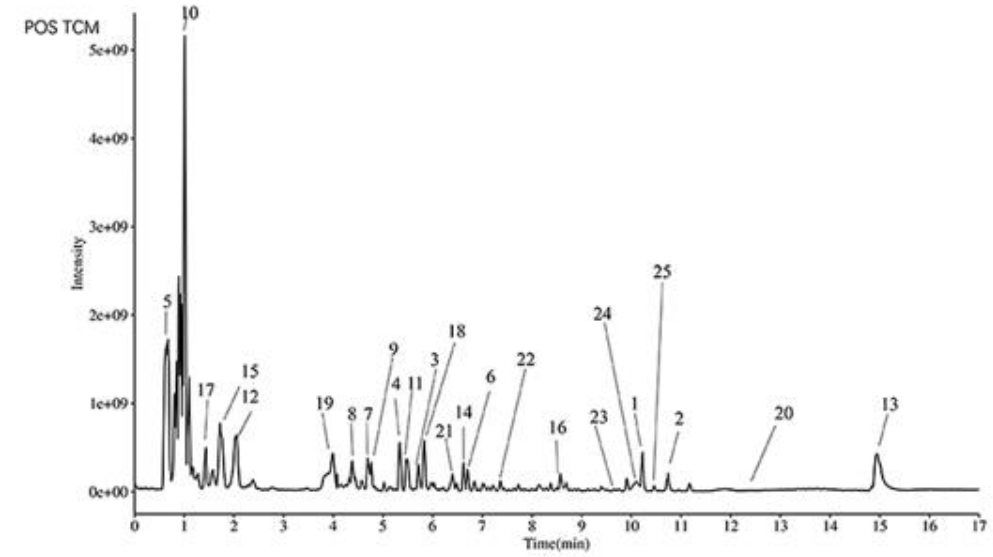

a)

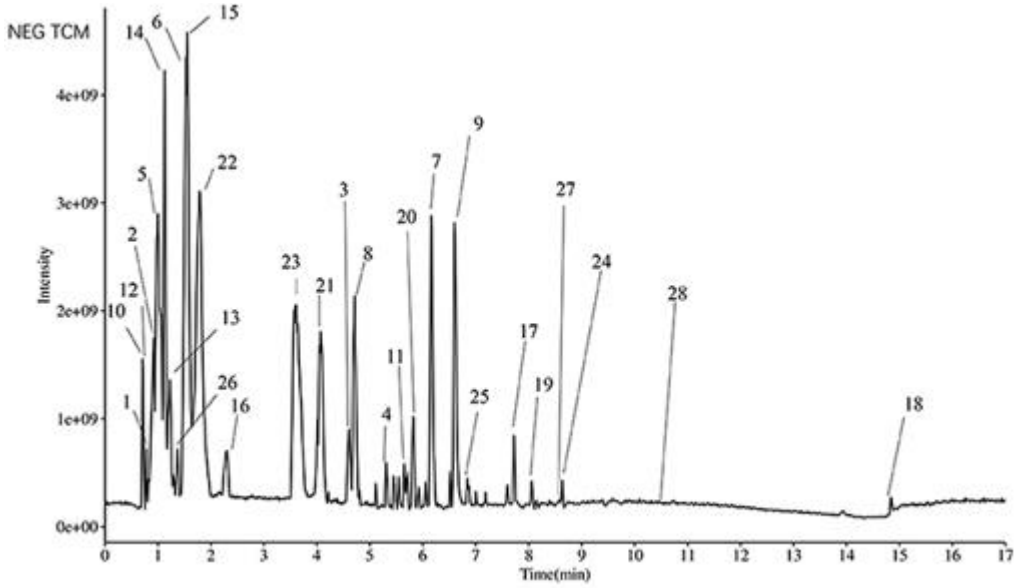

b)

Figure 2. The total ion chromatograms of XYSJD obtained via UHPLC-Q Exactive HFX-MS are shown in **Figure 3**: (a) represents the positive-ion mode, while (b) shows the negative-ion mode. To gain deeper insights into the mechanisms of XYSJD against TNBC, enrichment analyses were performed using Metascape. Gene Ontology (GO) analysis revealed that the main enriched biological processes included the positive regulation of apoptotic DNA fragmentation, among others **(Figure 3e)**. By integrating the top 10 hub genes identified previously, apoptosis-related genes such as BCL2 and TP53 were highlighted, suggesting that the bioactive compounds in XYSJD may exert therapeutic effects through the induction of TNBC cell apoptosis. This hypothesis was subsequently validated by targeted experiments. KEGG pathway enrichment further indicated that TNBC-related signaling pathways included the "Pathways in cancer" and the PI3K-Akt signaling pathway **(Figure 3f)**. Notably, AKT1 appeared as a high-degree hub gene, indicating that the PI3K/AKT1 signaling pathway may be a critical mediator of XYSJD's anti-TNBC activity.

Analysis of key gene expression and prognostic significance

Analysis using the TIMER database demonstrated that EZH2 and AKT1 expression levels were generally elevated in tumor tissues compared with adjacent normal tissues, particularly in breast cancer, thyroid cancer, and thymoma **(Figure 4a)**. Further evaluation using the GEPIA database revealed a positive correlation between EZH2 and AKT1 expression specifically in TNBC **(Figure 4b)**. Data from UALCAN and the GSE65194 dataset confirmed

that both genes were upregulated in TNBC tissues relative to other breast cancer subtypes and normal tissues **(Figures 4c and 4d)**. Additionally, higher expression of EZH2 and AKT1 was associated with more advanced disease stages **(Figure 4e)**, while elevated AKT1 expression also correlated with increased lymph node metastasis **(Figure 4f)**. Kaplan-Meier analysis of the GSE21653 dataset indicated that high AKT1 expression was significantly associated with poorer overall survival in TNBC patients, whereas EZH2 expression showed no significant impact on survival outcomes **(Figure 4g)**. These findings underscore the importance of AKT1 and EZH2 in TNBC progression and support their selection as key targets for subsequent molecular docking studies.

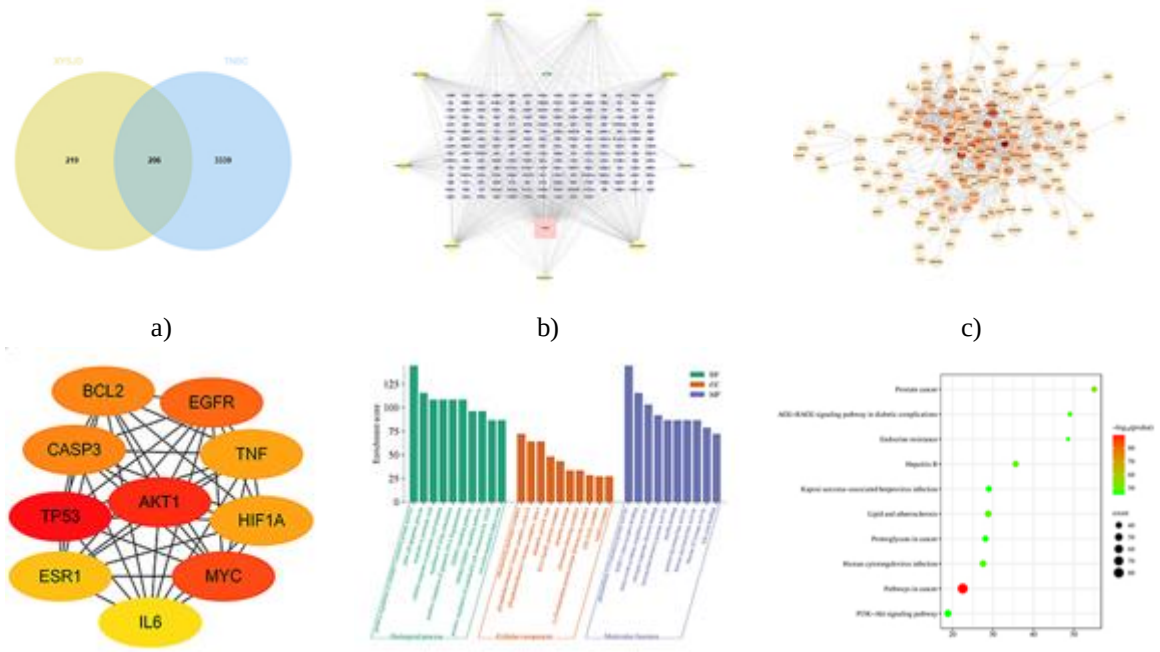

a) b) c)

d) e) f)

Figure 3. Network pharmacology analysis predicting the potential active components and mechanisms of XYSJD in TNBC. (a) Venn diagram showing the overlapping targets of XYSJD and TNBC;(b) network depicting the interactions between XYSJD compounds and TNBC targets; (c) protein-protein interaction (PPI) network, with node colors reflecting betweenness centrality—brighter colors indicate core genes; (d) the top 10 hub genes identified in the XYSJD-TNBC network; (e) Gene Ontology (GO) enrichment analysis, including biological processes (BP), cellular components (CC), and molecular functions (MF); (f) KEGG pathway enrichment analysis highlighting key signaling pathways involved.

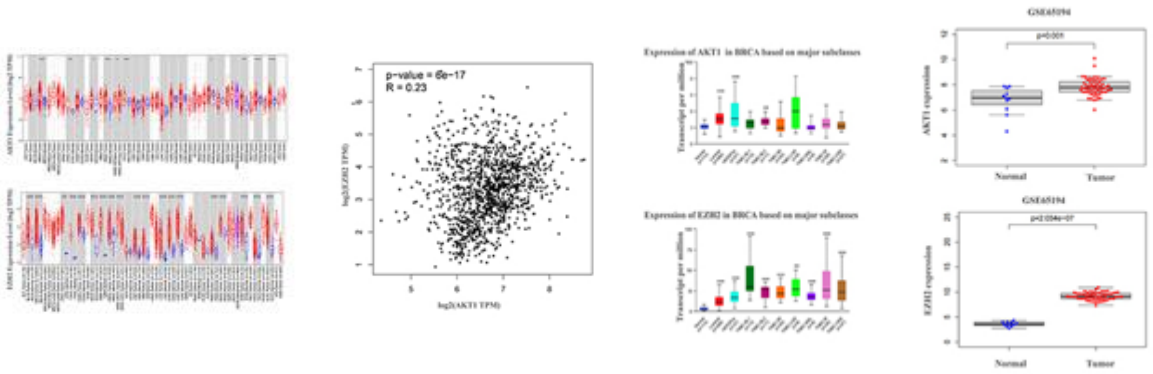

a) b) c) d)

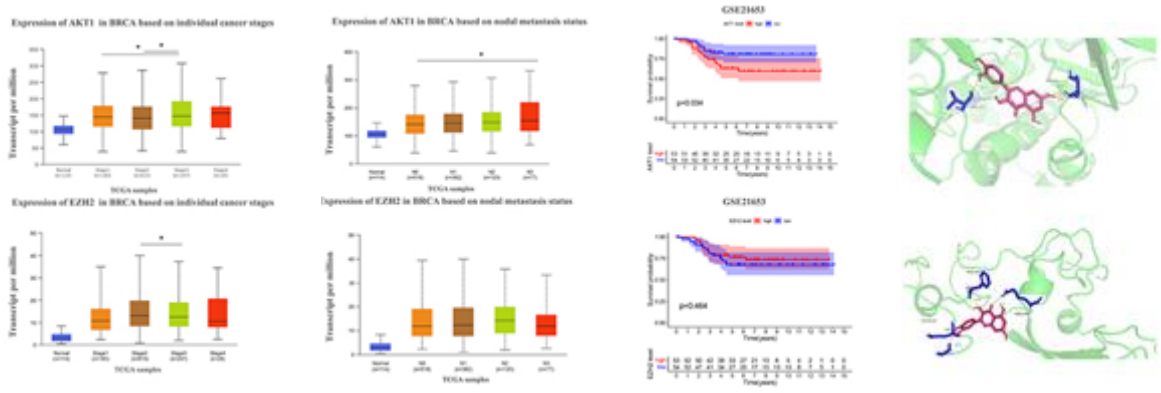

e) f) g) h)

Figure 4. Expression profiles, clinical relevance, prognostic significance of key target genes, and molecular docking validation. (a) Pan-cancer expression levels of AKT1 and EZH2 analyzed using TIMER (*p < 0.05, ***p < 0.001); (b) AKT1 and EZH2 expression in breast cancer subtypes, including TNBC, analyzed via UALCAN (*p < 0.05, **p < 0.01, ***p < 0.001); (c) Correlation analysis between AKT1 and EZH2 in TNBC using GEPIA2; (d) Differential expression of AKT1 and EZH2 in TNBC versus adjacent normal tissues from GSE65194; (e) Expression of AKT1 and EZH2 across different breast cancer stages analyzed via UALCAN (*p < 0.05); (f) Expression based on nodal metastasis status; (g) Kaplan-Meier survival analysis comparing high- and low-expression groups in GSE21653; (h) Molecular docking of quercetin (Que) with AKT1 and EZH2.

Molecular Docking Validation. Molecular docking revealed that quercetin exhibited strong binding affinities to the core target proteins AKT1 and EZH2, with binding energies of −9.6 and −8.3 kcal·mol⁻¹, respectively. As both values are ≤ −7.0 kcal·mol⁻¹, these results suggest a robust interaction between quercetin and the target proteins **(Figure 4h)**.

XYSJD-Containing Serum Inhibits TNBC Cell Proliferation. Treatment of MDA-MB-231 and MDA-MB-468 cells with XYSJD-containing serum for 48 and 72 h significantly suppressed cell proliferation at concentrations of 10%, 15%, and 20% compared with the control group (P < 0.01). The inhibitory effect increased with higher serum concentrations and longer exposure times. Although 5% serum did not significantly inhibit proliferation at 48 h, it effectively reduced TNBC cell growth after 72 h (P < 0.05; **(Figure 5a)**). These findings indicate that XYSJD-containing serum suppresses TNBC cell proliferation in a dose- and time-dependent manner.

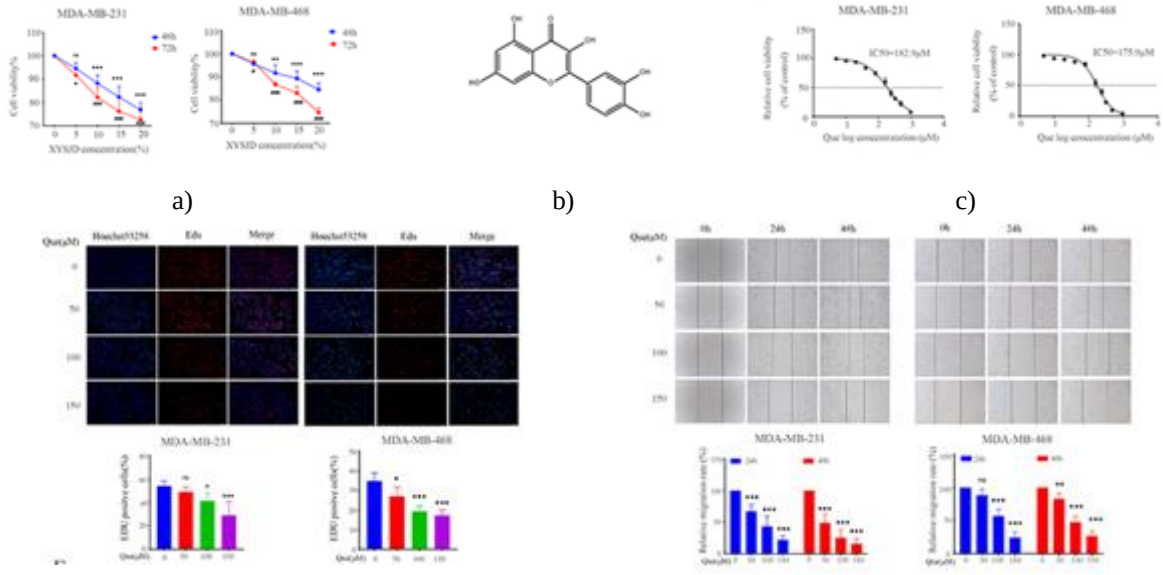

a) b) c)

d) e)

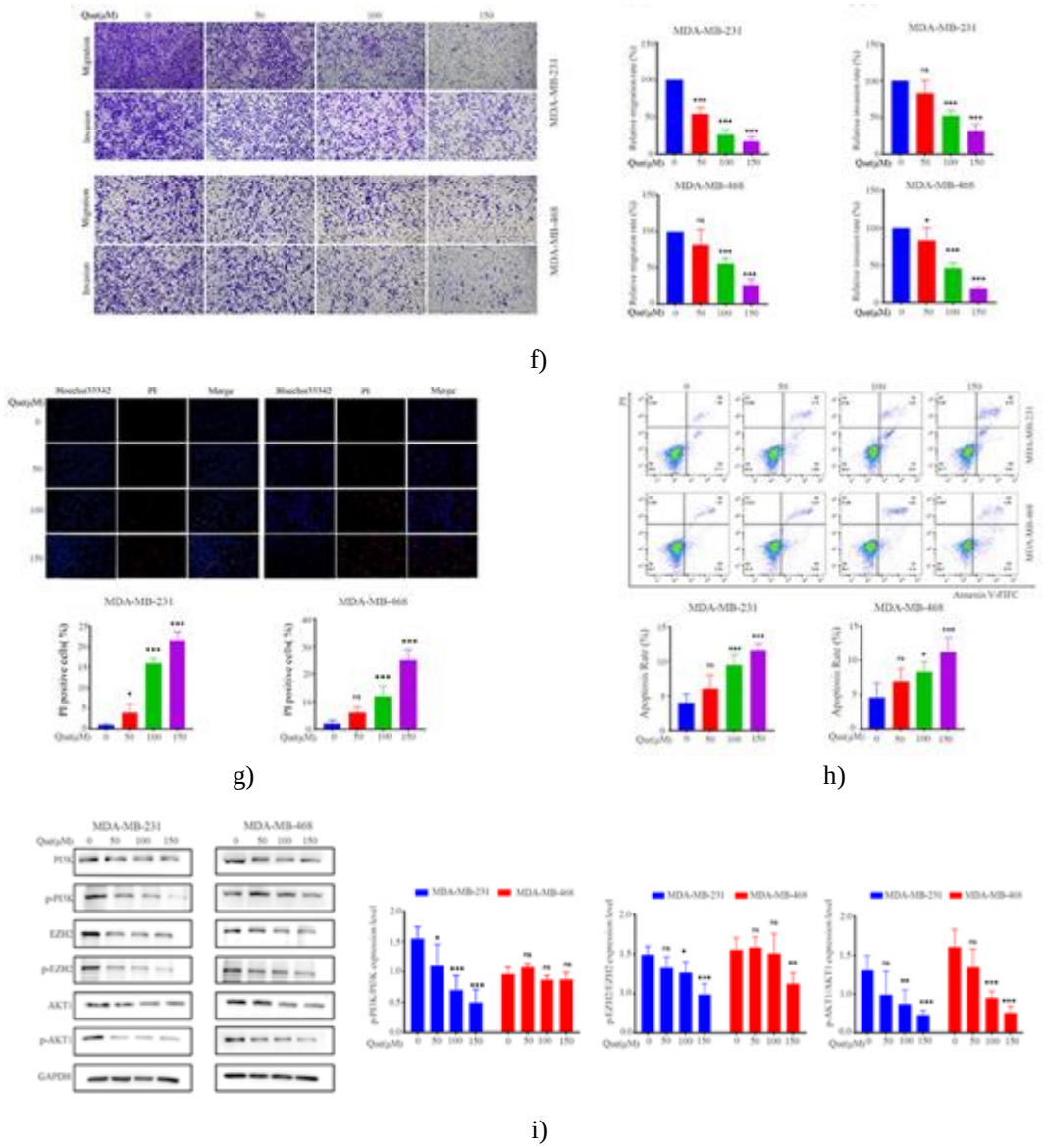

Figure 5. Quercetin (Que) suppresses TNBC cell proliferation and migration, induces apoptosis, and inhibits the EZH2/AKT1 signaling pathway. (a) CCK-8 assay showing the viability of TNBC cells treated with various concentrations of XYSJD (0%, 5%, 10%, 15%, 20%) for 48 and 72 h; (b) Molecular structure of quercetin; (c) CCK-8 assay measuring cell viability in Que-treated TNBC cells, normalized to the 0 μM control group; (d) EdU assay evaluating DNA replication in TNBC cells treated with Que (0, 50, 100, 150 μM) for 48 h. Red fluorescence represents EdU-positive cells; blue, nuclei (Hoechst 33258); (e) Wound healing assay and (f) Transwell assay assessing TNBC cell migration following 24 and 48 h Que treatment; (g) Hoechst/PI staining and (h) flow cytometry (Annexin V-FITC/PI) for apoptosis analysis; (i) Western blot analysis of PI3K, p-PI3K, EZH2, p-EZH2, AKT1, and p-AKT1 protein expression. Data are presented as mean ± SD (n = 5). *P < 0.05, **P < 0.01, ***P < 0.001 vs. control.

Quercetin Significantly Suppresses TNBC Cell Proliferation. Following 48 h of treatment with Que **(Figure 5b)**, the IC50 values for MDA-MB-231 and MDA-MB-468 cells were 182.9 μM and 175.9 μM, respectively **(Figure 5c)**. Based on these values, subsequent experiments utilized Que concentrations of 0, 50, 100, and 150 μM. EdU assays revealed a dose-dependent reduction in EdU-positive cells, with a marked decrease in proliferating cells at 100 and 150 μM compared with the control group **(Figure 5d)**. These findings indicate that Que effectively inhibits TNBC cell proliferation in a concentration-dependent manner.

Quercetin Inhibits TNBC Cell Migration. Wound healing assays demonstrated that the closure area of Que-treated TNBC cells (50, 100, 150 μM) decreased over 24 and 48 h relative to the control, indicating reduced

migration **(Figure 5e)**. Transwell assays further confirmed that Que treatment reduced the number of cells migrating and invading through the membrane in a dose-dependent manner **(Figure 5f)**.

Quercetin Promotes TNBC Cell Apoptosis. Hoechst/PI staining revealed increased nuclear fragmentation (blue, Hoechst) and PI-positive cells (red) at 100 and 150 μM Que, indicative of apoptosis **(Figure 5g)**. Flow cytometry analysis confirmed that apoptotic rates increased with higher Que concentrations compared with controls **(Figure 5h)**, demonstrating that Que induces apoptosis in a dose-dependent fashion.

Quercetin Inhibits the EZH2/AKT1 Signaling Pathway. Western blot analysis showed that Que treatment reduced p-EZH2/EZH2 and p-AKT1/AKT1 protein levels in a dose-dependent manner. While p-PI3K/PI3K levels decreased in MDA-MB-231 cells, no significant change was observed in MDA-MB-468 cells **(Figure 5i)**. Treatment with the pan-AKT activator SC79 restored phosphorylation of PI3K and AKT1, reversing Que-mediated inhibition in both cell lines **(Figure 6b)**. Overexpression of EZH2 was confirmed via RT-qPCR and Western blot **(Figure 6a)**, which led to increased p-AKT1/AKT1 levels in both TNBC cell lines. EZH2 overexpression enhanced p-PI3K/PI3K in MDA-MB-231 cells but not in MDA-MB-468 cells, suggesting that EZH2 may activate the AKT1 pathway independently of PI3K in MDA-MB-468. Combined treatment of EZH2 overexpression and Que reversed the inhibitory effect of Que on AKT1 **(Figure 6e)**. Collectively, these results indicate that Que suppresses TNBC cell proliferation, migration, and survival by inhibiting the EZH2/AKT1 signaling pathway.

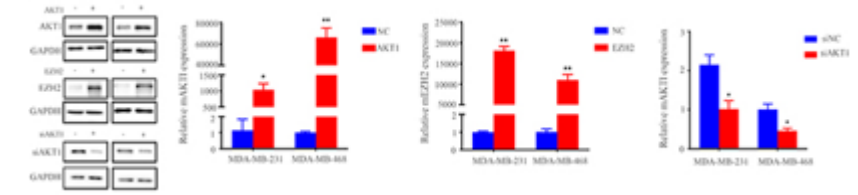

a)

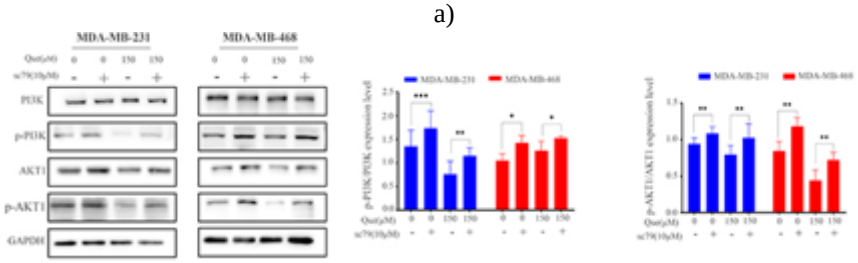

b)

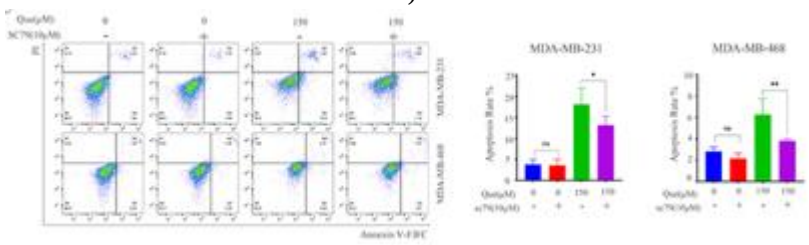

c)

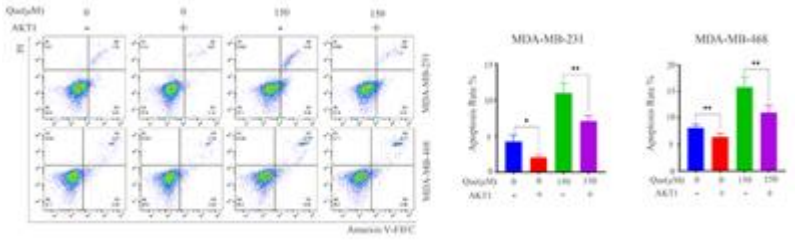

d)

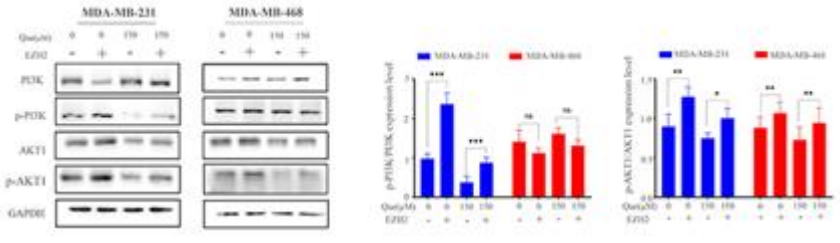

e)

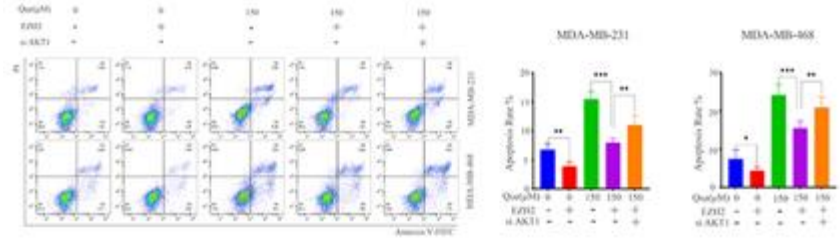

f)

Figure 6. Quercetin (Que) induces apoptosis in TNBC cells by inhibiting the EZH2/AKT1 signaling pathway. (a) Western blot and qPCR were used to confirm gene transfection efficiency; (b) Effects of Que and SC79 on the expression of PI3K/AKT1 pathway proteins; (c) Effects of Que and SC79 on TNBC cell apoptosis; (d) Effects of Que and AKT1 overexpression on apoptosis in TNBC cells; (e) Effects of Que and EZH2 overexpression on PI3K/AKT1 pathway protein levels; (f) Effects of Que combined with EZH2 overexpression and AKT1 silencing (siAKT1) on TNBC cell apoptosis. Data are presented as mean ± SD, n = 5, analyzed using GraphPad Prism 10.1.2. *P < 0.05, **P < 0.01, ***P < 0.001 vs. control.

Quercetin Promotes TNBC Cell Apoptosis via AKT1 Suppression. To validate that Que triggers apoptosis by inhibiting the AKT1 pathway, TNBC cells were treated with Que (150 μM) alongside AKT1 activation using SC79. Compared with the control group, SC79 alone slightly reduced apoptosis, but the difference was not statistically significant. In contrast, Que treatment markedly increased apoptosis, and co-treatment with Que + SC79 partially reversed this effect ($P < 0.05$; **(Figure 6c)**). Flow cytometry analysis further confirmed that AKT1 overexpression reduced apoptosis and counteracted Que-induced cell death ($P < 0.05$; **(Figure 6d)**). These results indicate that AKT1 activation suppresses apoptosis in TNBC cells, and Que induces apoptosis primarily by downregulating AKT1.

Quercetin Induces Apoptosis by Targeting the EZH2/AKT1 Pathway. AKT1 silencing efficiency was validated via RT-qPCR and Western blot, showing effective downregulation **(Figure 6a)**. Compared with controls, EZH2 overexpression reduced the apoptotic rate of TNBC cells ($P < 0.05$). Moreover, the apoptotic rate in the Que + EZH2 group was lower than in the Que-alone group ($P < 0.01$), but higher than in the EZH2 + siAKT1 + Que group ($P < 0.05$; **(Figure 6f)**). These findings suggest that EZH2 overexpression diminishes apoptosis, and Que induces TNBC cell apoptosis by inhibiting the EZH2/AKT1 signaling pathway.

XYSJD and Que Inhibit Breast Cancer Growth In Vivo. To evaluate in vivo efficacy, XYSJD and Que were tested in a human TNBC xenograft mouse model. Tumor volume and weight were significantly reduced in the Cisplatin, Que (80 mg/kg), and XYSJD groups compared with the control group **(Figures 7a–7c)**. Unlike Cisplatin-treated mice, body weights in the Que and XYSJD groups remained stable over 30 days **(Figure 7d)**. H&E staining of liver and kidney tissues revealed no significant toxicity in these groups **(Figure 7e)**. Western blot analysis of tumor tissues suggested that the anti-tumor effects of XYSJD and Que may involve inhibition of the PI3K/EZH2/AKT1 signaling pathway **(Figure 7f)**.

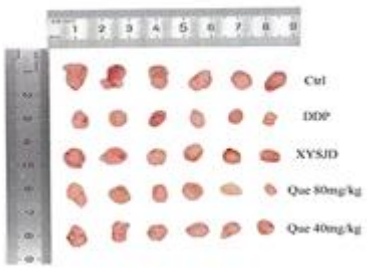

a)

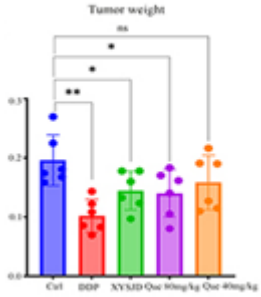

b)

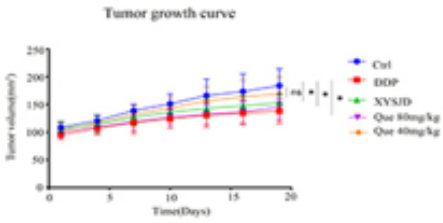

c)

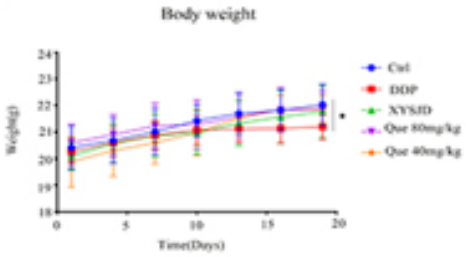

d)

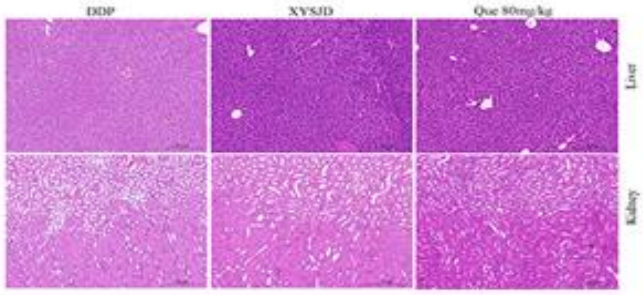

e)

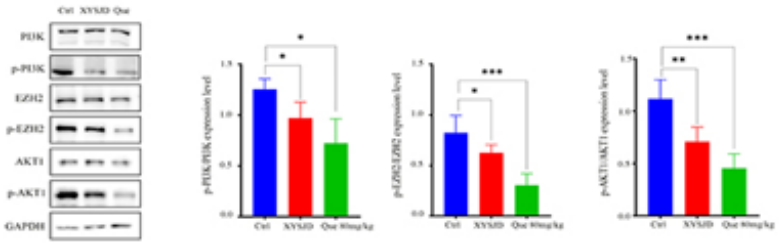

f)

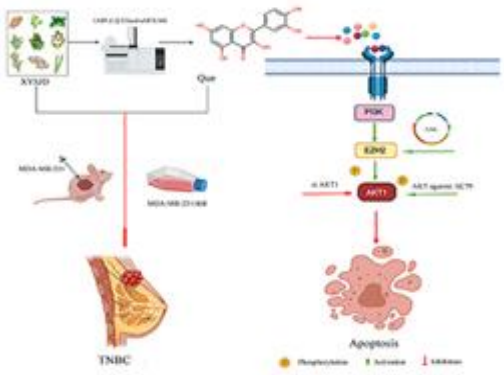

g)

Figure 7. XYSJD and Que suppress TNBC growth in nude mice. (a) Representative images of subcutaneous tumors from control, cisplatin, XYSJD, and Que-treated groups. (b) Tumor volume changes in each group

over time. (c) Tumor weights at the end of the experiment. (d) Body weights of mice during treatment. (e) H&E staining of liver and kidney tissues from each group (scale bar, 200 μm). (f) Western blot analysis of p-PI3K/PI3K, p-EZH2/EZH2, and p-AKT1/AKT1 expression in tumor tissues. (g) Proposed active components and molecular mechanism of XYSJD against TNBC. Data are presented as mean ± SD, n = 5; *P < 0.05, **P < 0.01, ***P < 0.001 vs. control.

Traditional Chinese Medicine (TCM) has a long-standing history and demonstrates promising therapeutic potential for triple-negative breast cancer (TNBC). According to TCM theory, TNBC falls within the category of "Ru Yan," a condition believed to be closely associated with blood stasis. Based on this pathological concept, XYSJD—known for its blood-activating and anti-tumor properties—has been developed and used clinically. Our study showed that serum containing XYSJD effectively suppressed the proliferation of TNBC cells. Considering the multi-component, multi-target, and multi-pathway nature of TCM formulas, we employed a combined approach using UHPLC-Q Exactive HFX-MS and network pharmacology to identify the major active constituents and mechanisms through which XYSJD acts against TNBC.

Following UHPLC-Q Exactive HFX-MS screening and evaluation of degree values within the "XYSJD–compound–target–TNBC" network, quercetin (Que) emerged as the most potent constituent of XYSJD and likely plays a key therapeutic role. Quercetin, one of the most common flavonoids, is recognized as a promising anticancer agent. Research indicates that it can modulate inflammatory responses, cause cell cycle arrest, inhibit angiogenesis, and suppress proliferation and migration in colorectal, liver, lung, and prostate cancers [38, 39]. It also influences apoptotic pathways and can induce tumor cell death [40]. Although quercetin exhibits beneficial effects against breast cancer in general [41], studies focusing specifically on its activity in TNBC remain limited. In our work, we demonstrated that quercetin markedly inhibited TNBC cell proliferation (CCK-8 and EdU assays), reduced migration and invasion (wound healing and transwell assays), and induced apoptosis (Hoechst/PI staining and flow cytometry). Furthermore, quercetin effectively suppressed TNBC tumor growth in vivo, with efficacy comparable to cisplatin but without significant hepatic or renal toxicity. These results collectively indicate that quercetin has robust therapeutic effects on TNBC both in vitro and in vivo.

Network pharmacology KEGG analysis identified the PI3K/AKT signaling pathway as a key target. Abnormal activation of this pathway is one of the most common genomic alterations across breast cancer subtypes [42]. The PI3K/AKT cascade regulates cell growth, survival, proliferation, metabolism, motility, and immune responses [43, 44], and its mutations are particularly common in TNBC [45]. Studies suggest that about 25% of primary TNBC tumors exhibit alterations in this pathway, with even higher rates in metastatic disease [46]. AKT, the primary downstream effector of PI3K signaling, exists in three isoforms—AKT1 (PKBα), AKT2 (PKBβ), and AKT3 (PKBγ) [47]—all implicated in TNBC progression [48]. Based on PPI and cytoHubba analyses, AKT1 was identified as a major target of XYSJD. Earlier research indicates that AKT1 promotes proliferation and modulates apoptosis in TNBC cells via cyclin D1 regulation [49]. It also plays roles in glucose metabolism and autophagy [50, 51], and may enhance lung metastasis by preventing TNBC cell apoptosis [52]. Clinical investigations have highlighted the therapeutic promise of AKT1 inhibitors [53].

PPI analysis also revealed EZH2 as another critical target of XYSJD. EZH2, a polycomb group protein involved in epigenetic regulation and cell memory, is frequently overexpressed in various cancers [54], a finding further supported by TIMER pan-cancer analysis. We observed that both AKT1 and EZH2 were significantly upregulated in TNBC tissues relative to adjacent normal tissues and were correlated with TNBC development. Previous studies reported that EZH2 can activate the PI3K/AKT pathway in breast cancer and promote proliferation and invasion by specifically stimulating AKT1 [55, 56]. However, the specific relationship between EZH2 and PI3K/AKT1 signaling in TNBC remains insufficiently defined. Thus, identifying agents capable of downregulating both EZH2 and AKT1 may offer a novel therapeutic strategy for TNBC.

Molecular docking results demonstrated that quercetin exhibits strong binding affinity toward AKT1 and EZH2. Western blot analysis further showed that increasing quercetin concentrations significantly decreased p-EZH2/EZH2 and p-AKT1/AKT1 levels in TNBC cells, consistent with predictions from network pharmacology. GO enrichment suggested that apoptosis induction is a principal biological process by which XYSJD may act against TNBC. Combining Hoechst/PI staining and flow cytometry, we confirmed that quercetin effectively triggers apoptosis in TNBC cells. Rescue experiments further supported that quercetin induces apoptosis by blocking the EZH2/AKT1 signaling axis.

Flow cytometry results showed that activating AKT1—either through the AKT1 activator SC79 or AKT1 overexpression—reduced apoptosis compared with controls. Moreover, the apoptotic rates in the Que + SC79 and Que + AKT1 overexpression groups were lower than those in the Que-only group, indicating that AKT1 activation mitigates quercetin-induced apoptosis. These findings confirm that quercetin triggers apoptosis in TNBC cells primarily through AKT1 suppression. Based on literature and our PPI findings, we hypothesized that EZH2 acts upstream of AKT1. Western blot results supported this, as EZH2 overexpression activated AKT1 signaling and counteracted quercetin's inhibitory effects on AKT1 **(Figure 6e)**. EZH2 overexpression also reduced apoptosis and reversed the pro-apoptotic effects of quercetin. Additionally, AKT1 knockdown further restored apoptosis in cells treated with both EZH2 overexpression and quercetin **(Figure 6f)**. Together, these findings confirm that quercetin induces TNBC cell apoptosis by inhibiting the EZH2/AKT1 pathway.

Conclusion

Overall, this study underscores the therapeutic value and safety of XYSJD and provides further evidence supporting its clinical application in TNBC treatment. Nonetheless, limitations remain. Given the complexity and diversity of TCM constituents and targets, the effects of quercetin alone cannot fully represent the complete anticancer profile of XYSJD. Importantly, XYSJD-containing serum demonstrated strong anti-proliferative effects on TNBC cells. Moving forward, we plan to integrate serum pharmacochemistry with network pharmacology to identify the active circulating components of XYSJD. Additionally, incorporating transcriptomics and metabolomics will allow deeper investigation into the multi-compound, multi-target, and multi-pathway mechanisms of XYSJD, providing valuable insights for future research.

Acknowledgments: None

Conflict of Interest: None

Financial Support: This study was sponsored by the Hubei University of Science and Technology PhD Start-up Fund Project Support (No.BK202422), Wuhan Municipal Health Commission Foundation (No.WZ21Q25), Wuhan Medical Science Research project (No. WX23Z16) and The foundation of the central hospital of Wuhan (No. 22YJ10).

Ethics Statement: Ethical approval was not required for the studies on humans in accordance with the local legislation and institutional requirements because only commercially available established cell lines were used. Animal experiment was approved by the formal review of experimental animal ethics at Huazhong university of Science and Technology. The IACUC approval number is IACUC-2022-3324. As for the bioinformatics experiment, the experiment was approved by Institutional Review Board of Hubei University of Science and Technology, and the IACUC approval number is IACUC-202410001.

References

1. Bray F, Ferlay J, Soerjomataram I, Siegel RL, Torre LA, Jemal A. Global cancer statistics 2018: GLOBOCAN estimates of incidence and mortality worldwide for 36 cancers in 185 countries. CA Cancer J Clin. 2018;68(6):394–424. doi:10.3322/caac.21492
2. Abramson VG, Lehmann BD, Ballinger TJ, Pietenpol JA. Subtyping of triple-negative breast cancer: implications for therapy. Cancer. 2015;121(1):8–16. doi:10.1002/cncr.28914
3. Lehmann BD, Pietenpol JA. Identification and use of biomarkers in treatment strategies for triple-negative breast cancer subtypes. J Pathol. 2014;232(2):142–50. doi:10.1002/path.4280
4. Yin L, Duan JJ, Bian XW, Yu SC. Triple-negative breast cancer molecular subtyping and treatment progress. Breast Cancer Res. 2020;22(1):61. doi:10.1186/s13058-020-01296-5
5. Lehmann BD, Bauer JA, Chen X, Sanders ME, Chakravarthy AB, Shyr Y, et al. Identification of human triple-negative breast cancer subtypes and preclinical models for selection of targeted therapies. J Clin Invest. 2011;121(7):2750–67. doi:10.1172/jci45014
6. Wolff AC, Hammond ME, Hicks DG, Dowsett M, McShane LM, Allison KH, et al. Recommendations for human epidermal growth factor receptor 2 testing in breast cancer: American Society of Clinical

Oncology/College of American Pathologists clinical practice guideline update. J Clin Oncol. 2013;31(31):3997–4013. doi:10.1200/JCO.2013.50.9984

7. Li Y, Zhang H, Merkher Y, Chen L, Liu N, Leonov S, et al. Recent advances in therapeutic strategies for triple-negative breast cancer. J Hematol Oncol. 2022;15(1). doi:10.1186/s13045-022-01341-0
8. Kumar H, Gupta NV, Jain R, Madhunapantula SV, Babu CS, Kesharwani SS, et al. A review of biological targets and therapeutic approaches in the management of triple-negative breast cancer. J Adv Res. 2023;54:271–92. doi:10.1016/j.jare.2023.02.005
9. Bianchini G, De Angelis C, Licata L, Gianni L. Treatment landscape of triple-negative breast cancer — expanded options, evolving needs. Nat Rev Clin Oncol. 2021;19(2):91–113. doi:10.1038/s41571-021-00565-2
10. Leon-Ferre RA, Goetz MP. Advances in systemic therapies for triple negative breast cancer. BMJ (Clinical Research Ed). 2023;381:e071674. doi:10.1136/bmj-2022-071674
11. Dent R, Trudeau M, Pritchard KI, Hanna WM, Kahn HK, Sawka CA, et al. Triple-negative breast cancer: clinical features and patterns of recurrence. Clin Cancer Res. 2007;13(15 Pt 1):4429–34. doi:10.1158/1078-0432.CCR-06-3045
12. Telang NT, Nair HB, Wong GYC. Growth inhibitory efficacy of Chinese herbs in a cellular model for triple-negative breast cancer. Pharmaceuticals (Basel). 2021;14(12):1318. doi:10.3390/ph14121318
13. Wu Q, Yan H, Kang Z. A review of traditional Chinese medicine for triple negative breast cancer and the pharmacological mechanisms. Am J Chin Med. 2024;52(04):987–1011. doi:10.1142/s0192415x2450040x
14. Pan J, Fu S, Zhou Q, Lin D, Chen Q. Modified xiaoyao san combined with chemotherapy for breast cancer: a systematic review and meta-analysis of randomized controlled trials. Front Oncol. 2023;13:1050337. doi:10.3389/fonc.2023.1050337
15. Chen WF, Xu L, Yu CH, Ho CK, Wu K, Leung GC, et al. The in vivo therapeutic effect of free wanderer powder (xiāo yáo săn, xiaoyaosan) on mice with 4T1 cell induced breast cancer model. J Tradit Complement Med. 2012;2(1):67–75. doi:10.1016/s2225-4110(16)30073-6
16. Liao H, Banbury LK, Leach DN. Effects and potential mechanisms of Danzhi Xiaoyao Pill on proliferation of MCF-7 human breast cancer cells in vitro. Chin J Integr Med. 2008;14(2):128–31. doi:10.1007/s11655-008-0128-y
17. Bai Y, Niu L, Song L, Dai G, Zhang W, He B, et al. Uncovering the effect and mechanism of jiawei xiaoyao wan in treating breast cancer complicated with depression based on network pharmacology and experimental analysis. Phytomedicine. 2024;128:155427. doi:10.1016/j.phymed.2024.155427
18. Wang J, Qi H, Zhang X, Si W, Xu F, Hou T, et al. Saikosaponin D from Radix Bupleuri suppresses triple-negative breast cancer cell growth by targeting beta-catenin signaling. Biomed Pharmacother. 2018;108:724–33. doi:10.1016/j.biopha.2018.09.038
19. Wang XZ, Xia L, Zhang XY, Chen Q, Li X, Mou Y, et al. The multifaceted mechanisms of paeoniflorin in the treatment of tumors: state-of-the-art. Biomed Pharmacother. 2022;149:112800. doi:10.1016/j.biopha.2022.112800
20. Lin PH, Chiang YF, Shieh TM, Chen HY, Shih CK, Wang TH, et al. Dietary compound isoliquiritigenin, an antioxidant from licorice, suppresses triple-negative breast tumor growth via apoptotic death program activation in cell and xenograft animal models. Antioxidants (Basel). 2020;9(3). doi:10.3390/antiox9030228
21. Jiang H, Li M, Du K, Ma C, Cheng Y, Wang S, et al. Traditional Chinese medicine for adjuvant treatment of breast cancer: taohong siwu decoction. ChinMed. 2021;16(1). doi:10.1186/s13020-021-00539-7
22. Wu S, Sun Z, Guo Z, Li P, Mao Q, Tang Y, et al. The effectiveness of blood-activating and stasis-transforming traditional Chinese medicines (BAST) in lung cancer progression-a comprehensive review. J Ethnopharmacol. 2023;314:116565. doi:10.1016/j.jep.2023.116565
23. Liu Z, Liu M, Liu M, Li J. Methylanthraquinone from Hedyotis diffusa WILLD induces Ca(2+)-mediated apoptosis in human breast cancer cells. Toxicol In Vitro. 2010;24(1):142–7. doi:10.1016/j.tiv.2009.08.002
24. Li M, Guo T, Lin J, Huang X, Ke Q, Wu Y, et al. Curcumin inhibits the invasion and metastasis of triple negative breast cancer via Hedgehog/Gli1 signaling pathway. J Ethnopharmacol. 2022:283. doi:10.1016/j.jep.2021.114689.
25. Luo H, Zhao L, Li Y, Xia B, Lin Y, Xie J, et al. An in vivo and in vitro assessment of the anti-breast cancer activity of crude extract and fractions from Prunella vulgaris L. Heliyon. 2022;8(11):e11183. doi:10.1016/j.heliyon.2022.e11183

26. Chen WJ, Tsai JH, Hsu LS, Lin CL, Hong HM, Pan MH. Quercetin blocks the aggressive phenotype of triple-negative breast cancer by inhibiting IGF1/IGF1R-mediated EMT program. J Food Drug Anal. 2021;29(1):98–112. doi:10.38212/2224-6614.3090
27. Srinivasan A, Thangavel C, Liu Y, Shoyele S, Den RB, Selvakumar P, et al. Quercetin regulates β-catenin signaling and reduces the migration of triple negative breast cancer. Molecular Carcinogenesis. 2016;55(5):743–56. doi:10.1002/mc.22318
28. Xu M, Xu Z, Xu Q, Zhang H, Liu M, Geng F, et al. UPLC-MS/MS method for the determination of 14 compounds in rat plasma and its application in a pharmacokinetic study of orally administered Xiaoyao Powder. Molecules. 2018;23(10):2514. doi:10.3390/molecules23102514
29. Ruan X, Zhang X, Liu L, Zhang J. Mechanism of Xiaoyao San in treating non-alcoholic fatty liver disease with liver depression and spleen deficiency: based on bioinformatics, metabolomics and in vivo experiments. J Biomol Struct Dyn. 2024;42(10):5128–46. doi:10.1080/07391102.2023.2231544
30. Li J, Zhang X, Guo D, Shi Y, Zhang S, Yang R, et al. The mechanism of action of paeoniae radix rubra-angelicae sinensis radix drug pair in the treatment of rheumatoid arthritis through PI3K/AKT/NF-κB signaling pathway. Front Pharmacol. 2023;14:1113810. doi:10.3389/fphar.2023.1113810
31. Kim Y, Park EJ, Kim J, Kim Y, Kim SR, Kim YY. Neuroprotective constituents from Hedyotis diffusa. J Natural Prod. 2001;64(1):75–8. doi:10.1021/np000327d
32. Gu X, Li Y, Mu J, Zhang Y. Chemical constituents of Prunella vulgaris. J Environ Sci (China). 2013;25(Suppl 1):S161–3. doi:10.1016/s1001-0742(14)60648-3
33. Liu Q, Li J, Gu M, Kong W, Lin Z, Mao J, et al. High-throughput phytochemical unscrambling of flowers originating from astragalus membranaceus (Fisch.) Bge. var. mongholicus (Bge.) P. K. Hsiao and Astragalus membranaceus (Fisch.) Bug. by Applying the Intagretive Plant Metabolomics Method Using UHPLC-Q-TOF-MS/MS. Molecules. 2023;28(16). doi:10.3390/molecules28166115
34. Rizzato G, Scalabrin E, Radaelli M, Capodaglio G, Piccolo O. A new exploration of licorice metabolome. Food Chem. 2017;221:959–68. doi:10.1016/j.foodchem.2016.11.068
35. Zhou Z, Chen B, Chen S, Lin M, Chen Y, Jin S, et al. Applications of network pharmacology in traditional Chinese medicine research. Evid Based Complement Alternat Med. 2020;2020(1):1646905. doi:10.1155/2020/1646905
36. Xu X, Zhang W, Huang C, Li Y, Yu H, Wang Y, et al. A novel chemometric method for the prediction of human oral bioavailability. Int J Mol Sci. 2012;13(6):6964–82. doi:10.3390/ijms13066964
37. Hu Q, Feng M, Lai L, Pei J. Prediction of drug-likeness using deep autoencoder neural networks. Front Genet. 2018;9:585. doi:10.3389/fgene.2018.00585
38. Lotfi N, Yousefi Z, Golabi M, Khalilian P, Ghezelbash B, Montazeri M, et al. The potential anti-cancer effects of quercetin on blood, prostate and lung cancers: an update. Front Immunol. 2023;14:1077531. doi:10.3389/fimmu.2023.1077531
39. Maugeri A, Calderaro A, Patanè GT, Navarra M, Barreca D, Cirmi S, et al. Targets involved in the anti-cancer activity of quercetin in breast, colorectal and liver neoplasms. Int J Mol Sci. 2023;24(3):2952. doi:10.3390/ijms24032952
40. Tang SM, Deng XT, Zhou J, Li QP, Ge XX, Miao L. Pharmacological basis and new insights of quercetin action in respect to its anti-cancer effects. Biomed Pharmacother. 2020;121:109604. doi:10.1016/j.biopha.2019.109604
41. Ezzati M, Yousefi B, Velaei K, Safa A. A review on anti-cancer properties of Quercetin in breast cancer. Life Sci. 2020;248:117463. doi:10.1016/j.lfs.2020.117463
42. Cancer Genome Atlas N. Comprehensive molecular portraits of human breast tumours. Nature. 2012;490:(7418):61–70. doi:10.1038/nature11412
43. Fruman DA, Chiu H, Hopkins BD, Bagrodia S, Cantley LC, Abraham RT. The PI3K pathway in human disease. Cell. 2017;170(4):605–35. doi:10.1016/j.cell.2017.07.029
44. Peng Y, Wang Y, Zhou C, Mei W, Zeng C. PI3K/Akt/mTOR pathway and its role in cancer therapeutics: are we making headway? Front Oncol. 2022;12. doi:10.3389/fonc.2022.819128
45. Costa RLB, Han HS, Gradishar WJ. Targeting the PI3K/AKT/mTOR pathway in triple-negative breast cancer: a review. Breast Cancer Res Treat. 2018;169(3):397–406. doi:10.1007/s10549-018-4697-y
46. Pascual J, Turner NC. Targeting the PI3-kinase pathway in triple-negative breast cancer. Ann Oncol. 2019;30(7):1051–60. doi:10.1093/annonc/mdz133

47. Manning BD, Toker A. AKT/PKB Signaling: navigating the Network. Cell. 2017;169(3):381–405. doi:10.1016/j.cell.2017.04.001
48. Basu A, Lambring CB. Akt isoforms: a family affair in breast cancer. Cancers. 2021;13(14):3445. doi:10.3390/cancers13143445
49. Johnson J, Chow Z, Napier D, Lee E, Weiss HL, Evers BM, et al. Targeting PI3K and AMPKalpha signaling alone or in combination to enhance radiosensitivity of triple negative breast cancer. Cells. 2020;9(5):1253. doi:10.3390/cells9051253
50. Yang W, Ju JH, Lee KM, Nam K, Oh S, Shin I. Protein kinase B/AKT1 inhibits autophagy by down-regulating UVRAG expression. Exp Cell Res. 2013;319(3):122–33. doi:10.1016/j.yexcr.2012.11.014
51. Lee JH, Liu R, Li J, Zhang C, Wang Y, Cai Q, et al. Stabilization of phosphofructokinase 1 platelet isoform by AKT promotes tumorigenesis. Nat Commun. 2017;8(1):949. doi:10.1038/s41467-017-00906-9
52. Johnson J, Chow Z, Lee E, Weiss HL, Evers BM, Rychahou P. Role of AMPK and Akt in triple negative breast cancer lung colonization. Neoplasia. 2021;23(4):429–38. doi:10.1016/j.neo.2021.03.005
53. Schmid P, Abraham J, Chan S, Wheatley D, Brunt AM, Nemsadze G, et al. Capivasertib plus paclitaxel versus placebo plus paclitaxel as first-line therapy for metastatic triple-negative breast cancer: the PAKT trial. J Clin Oncol. 2020;38(5):423–33. doi:10.1200/jco.19.00368
54. Kim KH, Roberts CWM. Targeting EZH2 in cancer. Nature Med. 2016;22(2):128–34. doi:10.1038/nm.4036
55. Liu Y, Yang Q. The roles of EZH2 in cancer and its inhibitors. Med Oncol. 2023;40(6). doi:10.1007/s12032-023-02025-6
56. Gonzalez ME, DuPrie ML, Krueger H, Merajver SD, Ventura AC, Toy KA, et al. Histone methyltransferase EZH2 induces akt-dependent genomic instability and BRCA1 inhibition in breast cancer. Cancer Res. 2011;71(6):2360–70. doi:10.1158/0008-5472.Can-10-1933